This article has been accepted for publication in a future issue of this journal, but has not been fully edited. Content may change prior to final publication. Citation information: DOI 10.1109/ACCESS.2019.2943752, IEEE Access

IEEE Access
Multidisciplinary : Rapid Review : Open Access Journal

Digital Object Identifier

Similarity-Based Chained Transfer Learning for Energy Forecasting with Big Data

YIFANG TIAN, LJUBISA SEHOVAC (Student Member, IEEE), AND KATARINA GROLINGER (Member, IEEE)
Department of Electrical and Computer Engineering, Western University, London, ON, N6A 5B9 CA (e-mail: {ytian285, lsehovac, kgroling}@uwo.ca)
Corresponding author: K. Grolinger (e-mail: kgroling@uwo.ca).

We acknowledge the support of the Natural Sciences and Engineering Research Council of Canada (NSERC), grant EGP 519910-2017

ABSTRACT Smart meter popularity has resulted in the ability to collect big energy data and has created opportunities for large-scale energy forecasting. Machine Learning (ML) techniques commonly used for forecasting, such as neural networks, involve computationally intensive training typically with data from a single building or a single aggregated load to predict future consumption for that same building or aggregated load. With hundreds of thousands of meters, it becomes impractical or even infeasible to individually train a model for each meter. Consequently, this paper proposes Similarity-Based Chained Transfer Learning (SBCTL), an approach for building neural network-based models for many meters by taking advantage of already trained models through transfer learning. The first model is trained in a traditional way whereas all other models transfer knowledge from the existing models in a chain-like manner according to similarities between energy consumption profiles. A Recurrent Neural Network (RNN) was used as the base forecasting model, two initialization techniques were considered, and different similarity measures were explored. The experiments show that SBCTL achieves accuracy comparable to traditional ML training while taking only a fraction of time.

INDEX TERMS Big Data, Deep Learning, Energy Forecasting, Gated Recurrent Units, Recurrent Neural Network, Smart Meters, Transfer Learning

I. INTRODUCTION

SMART meters are being installed in industrial, commercial, and residential buildings at increasing rates: presently there are over 70 million smart meters in the USA and over 96 million in China [1]. A number of smart meters together with their possibly frequent reading intervals results in a massive quantity of electricity consumption data. These Big Data have created new opportunities for analyzing energy use, designing demand-response programs, identifying savings opportunities, and measuring energy efficiency, but they also caused challenges related to processing such large data.

Energy forecasting has been attracting significant research interest because of the increased importance of preserving the environment, availability of smart meter data, and forecasting importance for both, retailers [2] and consumers [3]. Sensor-based energy forecasting relies on historical data from smart meters or other sensors, often in conjunction with meteorological information, to infer future energy consumption. Examples of Machine Learning (ML) techniques used for this task include Neural Networks (NN) [4], Support Vector Machine (SVM) [4], and their variants [5]. These ML techniques achieve good accuracy [1]; however, they are typically computationally complex and, with a high number of readings, it may be time-consuming to train a prediction model even for a single building/meter [6].

Recently, Recurrent Neural Networks (RNN) have outperformed other energy forecasting models [7]. An RNN is a type of NN where connections span adjacent time steps and form a directed graph along a temporal sequence. This makes them suitable for capturing time-dependencies and for dealing with time series data such as smart meter data. Because of spanning adjacent time steps, the total number of connections among neurons in an RNN is larger than in a traditional feed-forward neural network. Consequently, the number of weights to learning during training is increased, and so is the training time.

Many machine learning techniques, including RNNs, re-

This article has been accepted for publication in a future issue of this journal, but has not been fully edited. Content may change prior to final publication. Citation information: DOI 10.1109/ACCESS.2019.2943752, IEEE Access

quire training a forecasting model with historical data from a single building or a group of buildings to predict future consumption for that same building or the group of buildings. As training even a single forecasting model can be computationally expensive and time-consuming [6], repeating the same process for hundreds of thousands of meters becomes impractical or even infeasible.

Transfer learning has been identified as one of the open research areas in smart meter data analytics [1]; it is motivated by the fact that people can intelligently apply knowledge learned in the past to solve new problems in a new context in a faster and/or better way [8]. In traditional ML, models are built for a specific domain (e.g. specific smart meter) and task (e.g. energy prediction), and then used for the same domain and task (e.g. predict future consumption for the same meter). On the other hand, transfer learning aims to take advantage of knowledge gained on one domain/task and apply it to a different domain/task. Consequently, transfer learning has the potential to enable training machine learning models for many meters/buildings without the computational cost involved with training each model separately.

This paper proposes Similarity-based Chained Transfer Learning (SBCTL), a novel solution for building neural network-based forecasting models for a large number of smart meters. The model for the first meter is trained in a traditional manner using a Sequence-to-Sequence RNN; hyperparameters are optimized and weights learned using data from that meter. Next, the model is built for the meter with the energy consumption pattern the most similar to the pattern of the first meter, but the training process starts with the pre-trained model from the first meter. The process continues in a chain-like manner according to similarities in energy consumption patterns. Note that the SBCTL objective is not to improve accuracy for an individual meter, but to reduce training time when dealing with many meters. In the three experiments with different data sets (one with over 400 smart meters), SBCTL achieved accuracy comparable to traditional NN models while taking only a fraction of time.

The rest of the paper is organized as follows: Section II describes the background, Section III discusses the related work, Section IV presents SBCTL, Section V explains the experiments and corresponding results, and finally Section VI concludes the paper.

II. BACKGROUND

This section introduces the feed-forward and recurrent neural networks and presents transfer learning concepts.

A. FEED-FORWARD AND RECURRENT NEURAL NETWORKS

Feed-forward neural network (FFNN) consists of interconnected neurons organized in an input layer, hidden layer(s), and an output layer [9]. Neurons in each hidden layer are fully connected with neurons in the preceding and the subsequent layer; however, there are no connections among neurons in the same layer. The training process starts with initializing weights w between neurons to random values [9]; this initial state if referred to as the **seed**. The training samples are passed forward through the network and back-propagation is applied to minimize the objective function by updating the weights w [9]. An **epoch** refers to one forward pass and one backward pass of all training data; training typically requires a number of epochs for weights to converge. When the weights are updated using gradient descent, there is a possibility of getting stuck in a local minimum. To avoid this, training is often repeated by starting from different initial random states or seeds.

Recurrent neural networks (RNNs) are NN where connections between nodes form a directed graph along a temporal sequence [9]. RNN cells contain internal states capable of remembering information in sequential time steps, which makes them well-suited for time series forecasting tasks such as energy prediction. In traditional RNNs, the weights w are updated using back-propagation through time (BPTT) algorithm; however, this method suffers from the vanishing gradient problem [10]. To overcome this problem, the Long-Short Term Memory (LSTM) cell was designed [9]. To simplify LSTM while still maintaining the core functionality, the Gated Recurrent Unit (GRU) cell was introduced [11]. GRU cells compute reset gate r, update gate z, cell activation k, and hidden state h as [11]:

$$r_{[t]} = \sigma(W_{xr}x_{[t]} + b_{xr} + W_{hr}h_{[t-1]} + b_{hr}) \quad (1)$$

$$z_{[t]} = \sigma(W_{xz}x_{[t]} + b_{xz} + W_{hz}h_{[t-1]} + b_{hz}) \quad (2)$$

$$k_{[t]} = \tanh(W_{xk}x_{[t]} + b_{xk} + r_t \odot (W_{hk}h_{[t-1]} + b_{hk})) \quad (3)$$

$$h_{[t]} = (1 - z_{[t]}) \odot k_{[t]} + z_{[t]} \odot h_{[t-1]} \quad (4)$$

where σ is the sigmoid activation function, $\tanh$ is the hyperbolic $\tanh$ activation function, and $\odot$ represents element-wise multiplication. The input-hidden weight matrices are W_x's and hidden-hidden weight matrices are W_h's. Similarly, the b_x's and b_h's are the corresponding biases.

Sequence-to-Sequence (Seq2eqS) RNNs have been extensively used for language translation and recently have demonstrated success in energy forecasting [7]. They consist of two RNNs, an encoder and decoder RNN. This structure improves consecutive sequence prediction and allows Seq2Seq RNNs to have varying input and output lengths. Seq2Seq RNN can be used with LSTM or GRU cells.

B. TRANSFER LEARNING

Transfer learning is a machine learning approach where knowledge gained while performing a task in one domain is used to improve learning in a different domain or applied for a different task [8]. It is defined as follows [8]:

***Definition** 1 (Transfer Learning):* Given a source domain D_S and learning task T_S, a target domain D_T and learning task T_T, transfer learning aims to help improve the learning of the target predictive function $r_T(\cdot)$ in D_T using the knowledge in D_S and T_S, where $D_S \neq D_T$, or $T_S \neq T_T$. [8]

Here, a domain is a pair $D = \{F, P(X)\}$, where $F = \{f_1, ..., f_k\}$ is a feature space, X is a set of learning samples $X = \{x_1, ..., x_m\}$, and $P(X)$ is the marginal probability distribution of X. Domains are considered different if either marginal probability distributions or feature spaces are different.

Fig. 1 illustrates the difference between traditional machine learning and transfer learning. The traditional ML algorithms learn from a single domain for each model separately, whereas transfer learning uses the knowledge gained from multiple source domains to improve learning on the target domain. Different knowledge, such as instances, parameters, and relational knowledge, can be transferred across tasks and domains [8] .

In the energy forecasting with smart meter data, there is a single task (energy forecasting), but there are different domains: smart meters are considered different domains because they differ in energy consumption patterns and marginal probability distributions. SBCTL proposed here transfers weights and hyperparameters learned on the source domain (meter) to improve learning on the target domain. Thus, SBCTL belongs to the category of parameter transfer approaches.

III. RELATED WORK

Many approaches have been used for sensor-based energy forecasting; examples include fuzzy Bayesian [12], Support Vector Machine (SVM) [13], neural network [4] and ARIMA [14]. Tang *et al.* [12] were interested in predicting energy on an annual basis and they proposed probabilistic energy forecasting based on fuzzy Bayesian theory and expert prediction. Grolinger *et al.* [6] combined local learning with support vector regression (SVR) to reduce computation time while maintaining forecasting accuracy. Amber *et al.* [4] compared Multiple Regression (MR), Genetic Programming (GP), Artificial Neural Network (ANN), Deep Neural Network (DNN), and Support Vector Machine (SVM). Artificial Neural Network achieved better accuracy than the remaining four algorithms.

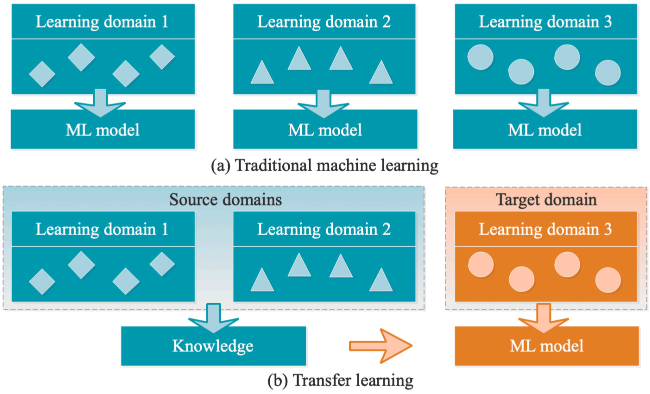

(a) Traditional machine learning

(b) Transfer learning

FIGURE 1: Traditional machine learning and transfer learning.

Several algorithms were combined to form ensemble learning models. Li *et al.* [15] proposed teaching-learning based optimization with artificial neural network for hourly energy prediction. Khairalla *et al.* [16] investigated Stacking Multi-Learning Ensemble (SMLE) model and combined Support Vector Regression (SVR), neural network, and linear regression learners. Baesmat *et al.* [5] proposed the weighted combination of ARIMA and RELM for city-level energy forecasting.

In recent years, recurrent neural networks have gained popularity in forecasting because of their ability to capture time-dependencies. Han *et al.* [17] proposed wind and photovoltaic power generation prediction based on copula function and LSTM network whereas Jiao *et al.* [18] designed multiple sequence LSTM RNN for non-residential load forecasting. Bouktif *et al.* [10] also used LSTM for energy forecasting but they combined it with genetic algorithm (GA) to find optimal time lags and the number of layers for the LSTM model. Standard LSTM was compared to Sequence-to-Sequence (Seq2Seq) architecture [19] and on one-minute time-step resolution datasets, Seq2Seq performed better. Similarly, in experiments performed by Sehovac *et al.* [7], Seq2Seq RNN also outperformed standard RNN.

As can be seen, the use of NN-based solutions has been quite popular [7], [10], [15]–[19] and recently Seq2Seq RNN provided increased prediction accuracy [7], [19]. Nevertheless, all the reviewed NN approaches focus on building a prediction model for a specific building or an aggregated load using historical data from that same building or the same aggregated load. In contrast, our work aims to reduce computation needed to create prediction models for a large number of smart meters taking advantage of transfer learning.

Transfer learning has been applied in different domains and for different tasks. For visual recognition, Zhu *et al.* [20] proposed a weakly-supervised cross-domain dictionary learning method. In Natural Language Processing (NLP), Hu *et al.* [21] improved mispronunciation detection with a deep neural network trained acoustic model and transfer learning-based Logistic Regression classifiers. In software engineering, Ma *et al.* [22] and Nam *et al.* [23] addressed cross-company software defect classification. In contrast to domain-specific solutions [20]–[23], Li *et al.* [24] aimed to develop a transfer learning model for a variety of applications and presented augmented feature representations for domain adaptation. Similarly, Mozafari *et al.* [25] were interested in transfer between different domains and proposed a SVM-based model-transferring method for heterogeneous domain adaptation. These works [20]–[25] focus on feature augmentation whereas our work belongs to the parameter transfer category as it transfers model parameters.

Parameter transfer is often found associated with pre-trained neural networks in computer vision [8]. Krizhevsky *et al.* [26] trained ImageNet, a large, deep Convolutional Neural Network (CNN) for classifying 1.2 million pictures. It is computationally expensive and time-consuming to train such a neural network with 650,000 neurons and 60 million parameters; nevertheless, once such a network is trained, it is a good foundation for other image classification problems. Menegola *et al.* [27] used pre-trained ImageNet to develop an approach for melanoma screening. Similarly, a pre-trained AlexNet, another deep CNN architecture, was used to detect pathological brain in magnetic resonance images [28]. These parameter-transfer approaches deal with image classification whereas SBCTL addresses forecasting with time series data.

In the energy domain, Mocanu *et al.* [29], Grubinger *et al.* [30], and Ribeiro *et al.* [31] applied transfer learning to provide prediction models for buildings with limited historical data by using data from other similar buildings with rich data sets. Wile those studies [29]–[31] aim to solve the limited data issue for target buildings, our objective is to reduce computation needed to train prediction models for a large number of buildings.

IV. SIMILARITY-BASED CHAINED TRANSFER LEARNING

This paper proposes the Similarity-Based Chained Transfer Learning (SBCTL) approach for building neural network-based energy forecasting models for a large number of buildings by applying transfer learning. The approach takes advantage of the initial neural network model trained with a single meter data to initialize training models for other smart meters. SBCTL is illustrated in Fig. 2 and details of each stage are described in the following subsections.

A. DATA PREPARATION

The smart meter data typically contain energy readings such as consumption and demand, and the corresponding date and time. If the reading intervals are different, all smart meter data are processed to make intervals between the readings the same. In the case of energy consumption, meters with finer reading granularity are converted to a coarser granularity by adding consumption readings.

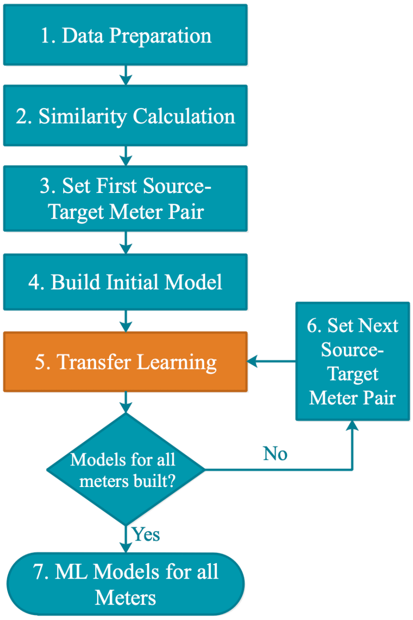
1. Data Preparation
2. Similarity Calculation
3. Set First Source-Target Meter Pair
4. Build Initial Model
5. Transfer Learning
6. Set Next Source-Target Meter Pair
Models for all meters built?
No
Yes
7. ML Models for all Meters

FIGURE 2: Similarity-Based Chained Transfer Learning (SBCTL).

Whereas feature selection is often considered in energy forecasting studies [32], SBCTL does not include it, as SBCTL is primarily designed for forecasting using smart meter data with limited number of features; in experiments we used only seven features. Nevertheless, when working with more features, SBCTL could be augmented by adding feature selection step.

Let us denote this meter data as $m_1, m_2, ..., m_k \in M$, where M is the set of all meters and k is the number of meters. This data is processed into two data sets: the similarity set D and the forecasting set G. Meter n data in D is denoted as d_n, $d_n \in D$, and the same meter data in G is denoted by g_n, $g_n \in G$. Although both d_n and g_n belong to the same meter, they are different in the number of features and time spans.

Similarity set D is created for calculation of similarities among energy consumption patterns recorded by different meters. It contains only energy consumption readings without any additional features because similarity is concerned solely with usage patterns. To capture quarterly and monthly patterns, D set must contain at least one year of energy readings. Each meter data d_n must start at the same date/time to ensure alignment of temporal patterns.

Forecasting set G, in addition to energy readings, contains other features generated from date and time such as day of the year, and weekday/weekend. Data pre-processing for this set depends on the type of the forecasting model used. As Sequence-to-Sequence (Seq2Seq) RNNs [7] have shown great results in energy forecasting for individual smart meters, they are used in SBCTL to build the initial model as well as to refine transferred models.

To enable the use of Seq2Seq RNN, data is prepared applying the sliding window techniques proposed by Sehovac *et al.* [7]. One input sample consists of a matrix $X \in \mathbb{R}^{T \times f}$, where T is the length of the input sequence or the number of time steps in a window and f is the number of features. Note that energy readings for all time steps of the input sequence are included as input features. If the input sample ends at time t, the corresponding target sequence consists of load values for time steps $t+1$ to $t+N$. This way, T time steps are used to predict the next N time steps ahead. The next sample is generated by sliding the window for one time step and repeating the same process.

The forecasting set is divided into training and test sets: first 80% of data is assigned for training and the last 20% for testing. This way, older data is used to train the model, and newer (test) data is used to evaluate and compare models. To capture monthly and quarterly patterns, the training set must contain at least one year of data; thus, the forecasting set G contains at least 15 months of data.

The complete SBCTL approach is given by Algorithm

Algorithm 1 SBCTL

```
1:  $Input$ : Set $M$ consisting of all meter data, initialization
2:  $Output$ : Models for all meters

3:  $D \leftarrow$ transform1 (M) // similarity set
4:  $G \leftarrow$ transform2 (M) // forecasting set (training)
5:  $D \leftarrow$ normalization($D$)
6:  $L(d_i, d_j) \leftarrow$ similarity $(d_i, d_j)$, for all $d_i, d_j \in D, i < j$
7:  $T \leftarrow M$ // initialize target set
8:  $S \leftarrow \{\}$ // initialize source set

9:  $if$ initialization == A // From the most similar pair
10:     $(p, q) \leftarrow \arg\min_{i,j} L(d_i, d_j),\ for\ d_i, d_j \in D, i < j$
11: $elseif$ initialization == B // From the center
12:     $d_{center} \leftarrow mean(d_i),$ for $d_i \in D$
13:     $p \leftarrow \arg\min_{i} L(d_i, d_{center}),$ for $d_i \in D$
14:     $q \leftarrow \arg\min_{i} L(d_p, d_i),$ for $d_i \in D, i \neq p$

15: $m_p^m \leftarrow$train initial model for $m_p$ with $g_p$ data
16: $S = S \bigcup \{m_p\}$   // add to source
17: $T = T/S$          // remove from target

18: $while\ T \neq \{\}\ do$
19:     $m_q^m \leftarrow$ transfer learning $(m_p^m)$ with $g_q$ data
20:     $S = S \bigcup \{m_q\}$   // add to source
21:     $T = T/S$          // remove from target
22:     $if\ T \neq \{\}$
23:         $(p, q) \leftarrow \arg\min_{i,j} L(d_i, d_j),\ for\ m_i \in S, m_j \in T$
24: $Return$ : Models for all meters $\{m_1^m, m_2^m ... m_k^m\}$
```

1. For simplification, in the algorithm, G refers to only the training part of the forecasting set. The approach starts with data preparation, specifically by creating sets D and G, lines 3 and 4, and continues with the steps described in the remaining subsections.

B. SIMILARITY CALCULATION

Similarity calculation gives a numeric value to similarities between each possible pair of meters. Here, we are interested in energy patterns and not in the actual values of energy consumption. Therefore, all values from similarity data set D are first scaled to bring them to the same range (line 5 in Algorithm 1). Min-max normalization is performed for each meter separately resulting in each meter values in [0,1] range.

Next, similarity between all pairs of meters is calculated (line 6, Algorithm 1); four different metrics are considered. Euclidean, Cosign, and Manhattan distances between meter i and j are calculated as follows:

$$L_{Eucl}(d_i, d_j) = \sqrt{\sum_{t=1}^{N} (d_i^t - d_j^t)^2} \tag{5a}$$

$$L_{Cosign}(d_i, d_j) = 1 - \frac{\sum_{t=1}^{N} (d_i^t d_j^t)}{\sqrt{\sum_{t=1}^{N} (d_i^t)^2} \sqrt{\sum_{t=1}^{N} (d_j^t)^2}} \tag{5b}$$

$$L_{Manh}(d_i, d_j) = \sum_{t=1}^{N} |(d_i^t - d_j^t)| \tag{5c}$$

$$for\ d_i, d_j \in D, i < j \tag{5d}$$

The fourth metrics considered is Dynamic Time Warping (DTW) distance [33]. DTW was selected because it is capable of measuring similarity between the two temporal sequences which may vary in speed. A well known example of a DTW application is automatic speech recognition where DTW is capable of handling different speaking speeds. In energy data, DTW could potentially capture peak shifts or prolonged peak periods. To control how much the sequences can be "warped" for the comparison calculation, a locality constraint referred to as the **window** is commonly added. In our work, experiments consider different window sizes in order to examine their impact on the forecasting accuracy.

For k number of meters, the outcome of the similarity calculation is a $k * k$ upper oblique matrix; this similarity matrix is denoted as S_{im}^{k*k}. The lower the distance value between two meters, the more similar are the meters.

C. SET FIRST SOURCE-TARGET METER PAIR

The main idea behind SBCTL is to use a similarity measure to determine the source and target meters for the transfer process. To start with, none of the meters have an associated prediction model. Therefore, as indicated in lines 7 and 8, Algorithm 1, all meters belong to the target set T and the source set S is empty. Throughout the process, the target set will always have only the meters that do not yet have the corresponding prediction model and the source set will contain meters with an already trained model. Two different initialization techniques are considered:

Initialization A**:** Starting from the pair of the most similar meters. As indicated in Algorithm 1, line 10, the two meters that correspond to the minimum value in the similarity matrix S_{im}^{k*k} are assigned as a starting source-target pair (p, q). Either one of the two meters in the pair can be set as the source p; experiments will evaluate switching p and q in the first source-target pair.

Initialization B**:** Starting from the meter that is the closest to the center. First, the center is calculated from the similarity data set D (Algorithm 1, line 12). For each time step t in the similarity set, the arithmetic mean d_{center}^t is calculated as:

$$d_{center}^t = \frac{1}{k} \sum_{i=1}^{k} d_i^t \tag{6}$$

This article has been accepted for publication in a future issue of this journal, but has not been fully edited. Content may change prior to final publication. Citation information: DOI 10.1109/ACCESS.2019.2943752, IEEE Access

where k stands for the number of meters and d_i^t is a reading from meter i at time step t.

The meter that is the closest to this center C according to selected similarity metrics is chosen as the initial meter p (Algorithm 1, line 13). The meter that is the most similar to the initial meter p is selected as meter q (Algorithm 1, line 14).

D. BUILD INITIAL MODEL

This step is responsible for building the first prediction model which will serve as a starting point for the transfer learning. The initial model is built for the meter that was assigned as the source p (line 10 or 13, Algorithm 1). As indicated in line 15, the initial model for meter m_p is trained using forecasting data set g_p.

SBCTL is designed for NN-based algorithms; therefore, all models, including the initial one, must be built using a same NN approach. Specifically, a Seq2Seq RNN [7] is used because of its recent success. A Seq2Seq RNN [7] consists of an encoder RNN and decoder RNN as illustrated in Fig. 3. An input sequence $x_{[1]}, ..., x_{[T]}$ is passed through the encoder RNN to obtain an encoded representation of the input vector referred to as the context vector ($\vec{c}$). The decoder RNN extracts information from this context vector at each output time step to obtain the prediction sequence $\{\hat{y}_{[1]}, ..., \hat{y}_{[N]}\}$. The initial input for the decoder RNN is the context value $\hat{y}_{[0]}$ derived from the context vector.

This first model is trained in a traditional way: weights are initialized to random values and model is trained for a sufficient number of epochs ensuring that weights converge. To avoid local minimum, the process is repeated starting with a different set of random initial values referred to as *seeds*. The best model among all runs with different seeds is chosen for forecasting and used in the following SBCTL steps.

NN hyperparameters such as a number of layers and neurons, are also tuned in this step by splitting the training data into the training and validation sets; model selection is done on the validation set. After tuning hyperparameters for the initial model, they remain the same throughout the transfer learning and for all meter models. In contrast, the weights learned during the initial model training are used as a starting point for other models, but the weights do change.

The result of the training and tuning is the prediction model for meter p denoted as m_p^m (Algorithm 1, line 15). Note that m_p indicates meter data for the meter p and m_p^m denotes the trained model for the same meter p. Because meter p now has the forecasting model, it is added to the set of source meters S, line 16, and removed from the set of target meters T, line 17. This initial model is now available for transfer learning.

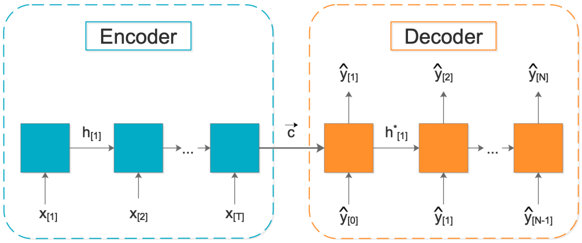

FIGURE 3: Sequence-to-Sequence Recurrent Neural Network.

E. TRANSFER LEARNING

The initial model m_p^m is used as a seed for building all other prediction models through transfer learning. The assumption is that if the meters share some similarity, so should their trained models. Thus, if we use the initial prediction model as a starting point for building the model for the most similar meter, the training should be reduced.

The meter to transfer knowledge to is the q meter from the (p, q) pair. Because the pair is determined according to similarities, SBCTL ensures that the transfer happens between more similar meters. As indicated in line 19, existing model m_p^m trained previously for meter p and with data set g_p, is now used as a starting point for building meter q model. Model m_p^m continues training, but now with the target meter data g_q to obtain model m_q^m. Network structure and hyperparameters determined during training for the first meter remain the same throughout the transfer learning and for all forecasting models. The weights from the source meter model m_p^m are transferred to the target meter q, but they change through training with the target meter data g_q. The number of training epoch needed for the weights to converge is lower because the training starts from the pre-trained weights.

If the two meters from the pair are very similar, the transferred model, without any training with the target meter data, may already provide reasonable accuracy: we refer to transfer without additional training as epoch 0. The evaluation will explore how many epochs with target data are needed to achieve comparable accuracy to traditional NN training.

The result of the training with the transferred model is the new model m_q^m, line 19. Next, as meter q now has the forecasting model, it is added to the set of source meters S, line 20, and removed from the set of target meters T, line 21. This additional model now is available for transfer learning.

If there are still meters that do not have a corresponding prediction model, in other words, if the target set T is not empty (lines 22 and 18), the SBCTL will proceed to Set Next Source-Target Meter Pair step. If forecasting models are trained for all meters, the SBCTL process is completed.

F. SET NEXT SOURCE-TARGET METER PAIR

In this step, the next source-target meter pair (p, q) is selected for transfer learning. As indicated in the algorithm's name SBCTL, the processed is chained: building the next forecasting model depends on the previously built models. In each loop of the chained process, the forecasting model will always be transferred from one meter in the source set S to one meter in the target set T.

To determine which model should be trained next, the similarity distances calculated in line 6 are used. Because the transfer needs to happen from an already trained model, we are interested in finding a meter from the target set T that is the most similar to any meter in the source set S. Thus, line 23 in Algorithm 1 finds the pair with minimum distance L under the constraint that $m_p \in S$ and $m_q \in T$. The model will be transferred from from m_p to m_q.

When the next source-target pair (p, q) is set (line 23), SBCTL continues to transfer learning, line 19, described in subsection IV-E.

G. ML MODELS FOR ALL METERS

This is the final output of the SBCTL process. As indicated in line 18, the transfer learning process completes when the target set is empty $T = \{\}$ and all meters belong to the source set S. The algorithm results are the trained ML models for all meters $m_1^m, m_2^m ... m_k^m$.

V. EVALUATION

This section introduces the evaluation process, describes the three experiments with different data sets, and discusses the findings. Experiments one and two consider smaller data sets consisting of 7 and 19 meters, respectively. A small number of meters in these two experiments allows for detailed examination of the transfer process as well as for accuracy comparison for each individual meter. On the other hand, the third data set consisting of 456 meters allows for evaluation at scale and demonstrates SBCTL forecasting accuracy and time savings with larger data. The used hardware was different for each data set and reflects the increase of data set size.

All of the experiments applied SBCTL with initializations A and B. Also, Euclidean, Cosine, Manhattan, and DTW distance with window size of 3, 6, 12, and 24 were evaluated. SBCTL was implemented using Python with Pandas and PyTorch libraries. GRU cells were used in Seq2Seq RNN because they achieved higher accuracy than LSTM in single meter forecasting [7]. The hyper-parameters used for the initial model as well as for all other models were: Hidden dimension size = 64, Batch size = 256, Epochs = 10, Optimizer = Adam, Learning rate = 0.001, Encoder size = 8 and Decoder size = 4.

A. EVALUATION PROCESS

For each meter in each experiment, SBCTL was compared to the traditional machine learning:

- **Traditional ML**. For each meter, an individual Seq2Seq RNN model was trained using that meter training data. The process was repeated with 10 seeds and the model with the best MAPE was selected for comparisons. As a large number of models from the two experiments converged around the 10th epoch, the comparison was carried out with 10 epochs. For each epoch, the model was tested on the test set and accuracy was recorded.
- **SBCTL**. The models are built using SBCTL approach. In each experiment, the first model is built using the traditional approach. All other models are built using SBCTL transfer learning and only trained for 5 epochs because the training starts from the pre-trained weights. For each epoch, including 0 epoch (no training on target), the models were tested on the test set and accuracy was recorded.

To evaluate model accuracy, Mean Absolute Error (MAE) and Mean Absolute Percentage Error (MAPE) were selected because of their frequent use in energy forecasting studies [1]:

$$\text{MAE} = \frac{1}{N'} \sum_{t=1}^{N'} |y_t - \hat{y_t}| \tag{7}$$

$$\text{MAPE} = \frac{100\%}{N'} \sum_{t=1}^{N'} \left| \frac{y_t - \hat{y_t}}{y_t} \right| \tag{8}$$

where y is the actual value, $\hat{y}$ is the predicted value, and N' stands for the number of test set samples.

Other metrics such as Mean Absolute Error (MSE) and Root Mean Square Error (RMSE) were also calculated in the experiments, but they are not shown here as they exhibit the same patterns as MAE and MAPE.

B. EXPERIMENT ONE

This experiment was performed on MacBookPro with 2.9 GHz Intel Core i7 processor and 16 GB LPDDR3 memory.

1) Data set

Experiment one used a private data set from seven real-world meters measuring commercial buildings energy consumption in 15 min intervals. This data set, as well as data sets in remaining experiments, consist of reading date/time with corresponding energy consumption. For experiment one, the total number of readings was: 4 readings in one hour × 24 hours × 487 days = 46,752 for each meter.

Daily consumption profiles for meters 4 and 5 are depicted in figures 4 and 5, respectively. Meter 4 shows different patterns for weekend and weekdays, whereas meter 5 displays similar patterns for all days (no weekday/weekend distinction) but different from meter 4. Although the patterns and average consumption are different among meters, SBCTL is able to transfer knowledge among the models.

2) Experiment

The similarity set D contained one year of energy readings without any additional features. The forecasting set G contained additional generated features (month and day of the year, day of the month, day of the week, weekend, hour, season, holiday) and included readings from all 487 days. A few samples from G are shown in Table 1.

In Similarity Calculation step, the usage readings were normalized and the distance matrices were calculated. Set First Target-Source Meter Pair step with initialization A selected meters 2 and 4 as the meters with the smallest distance; thus, the first pair can be $(2, 4)$ or $(4, 2)$. Experiments

TABLE 1: Example Data from Forecasting Data Set

Index	Month	Day of Year	Day of Month	Weekday	Weekend	Holiday	Hour	Season	Usage (kW)
0	6	158	6	0	0	0	0	3	881.36
11661	10	279	5	2	0	0	11	4	1507.47
42978	8	239	27	6	1	0	16	3	983.60

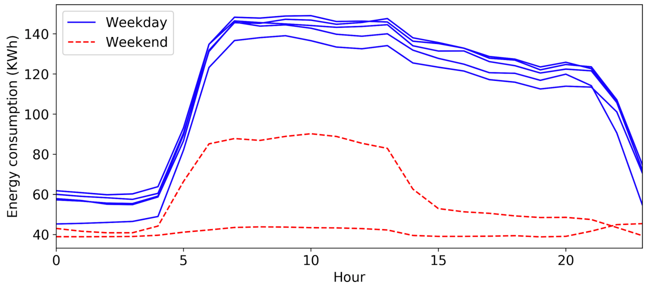

FIGURE 4: Daily load profile - meter 4.

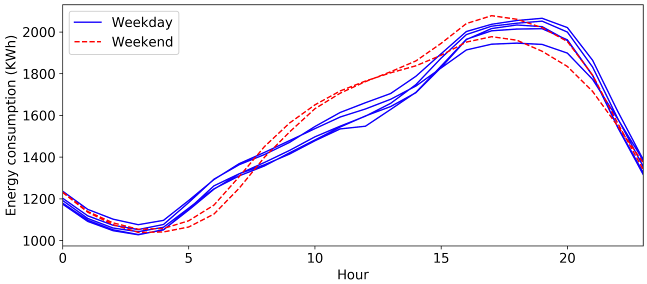

FIGURE 5: Daily load profile - meter 5.

were performed for both transfer paths $(2, 4)$ and $(4, 2)$. With initialization *B*, the initial meter was meter 4, and the transfer path was the same as for initialization *A* with 4 as the starting meter. Here, the following steps are described assuming $(4, 2)$ order. The experiments were performed for both transfer paths $(2, 4)$ and $(4, 2)$.

Next, in Build Initial Model step, the model for meter 4 is trained with the training part of g_4. After the best model m_4^m for meter m_4 was completed, m_4 was removed from target set T and added to source set S.

In Transfer Learning step, model m_4^m was transferred to meter 2 making m_2^m. The model m_2^m was first tested directly on the test set of g_2 (transfer 0 epoch) and then trained with the training set of g_2 for 5 epochs. Upon completed training, m_2 was removed from the target set T and added to source set S.

Next, Set Next Source-Target Meter Pair step determines the order of remaining transfers. In this experiment, initialization *A* with the first meter 4 and initialization *B* shared the same chained transfer path presented in Table 2. The first row indicates transfer from meter 4 to meter 2; the second row shows transfer from meter 2 to 7, and so on. The pairs were chosen to satisfy the condition of minimum distance value under constraints that one meter belongs to the source set S and one to the target set T as indicated in line 18, algorithm 1. The process ends when all meters have the corresponding prediction model.

3) Result

The main objective of the experiments is to compare SBCTL accuracy with that of traditional machine learning when the model is trained for each meter individually. Thus, SBCTL is deemed successful if it is able to achieve similar accuracy to traditional ML but with reduced computation.

Fig. 6 compares the accuracy of SBCTL and traditional ML in terms of MAE for the six meters. Meter 4 is not included because it was the initial meter and, thus, follows the traditional ML training. The horizontal dashed line indicating the SBCTL accuracy at 5 epochs is included to ease visual comparison. It can be seen that when the model is transferred without additional training (epoch 0), MAE is relatively high. Nevertheless, MAE drops sharply in epochs 1 and 2, and after 5 epochs, 5 out of 6 meters achieve better accuracy than the traditional ML and the sixth meter m_6 achieves MAE within 0.01 difference. Moreover, after 3 epochs, all meters achieve accuracy comparable to traditional ML.

In addition to accuracy, it is important to compare computational cost; thus, the average elapsed time, standard deviation, and variance for traditional ML and SBCTL are shown in Table 3. For SBCTL, the initial meter 4 is not included as it is trained in a traditional way. It can be observed that for SBCTL with three epochs, time was reduced to 10.48s from 365.47s achieved with traditional ML what is about 97% reduction. Note that traditional training was repeated with 10 different seeds (initializations) while the SBTCL starts from the single initial state transferred from an already trained meter.

For the initial pair or meters (4,2), two paths are possible;

TABLE 2: Experiment One: Chained Transfer Path

Step	Source Meter	Target Meter	Euclidean Distance
1	m_4	m_2	135.2
2	m_2	m_7	135.5
3	m_4	m_6	160.4
4	m_4	m_1	202.9
5	m_1	m_5	198.4
6	m_5	m_3	264.0

TABLE 3: Experiment 1: Average Training Time

	Traditional			SBCTL	epoch		
	10	0	1	2	3	4	5
Time (s)	**365.47**	0	3.53	7.00	**10.48**	14.09	17.64
Std.Dev	0.13	0	0.07	0.08	0.11	0.21	0.32
Variance	0.018	0	0.005	0.006	0.012	0.046	0.100

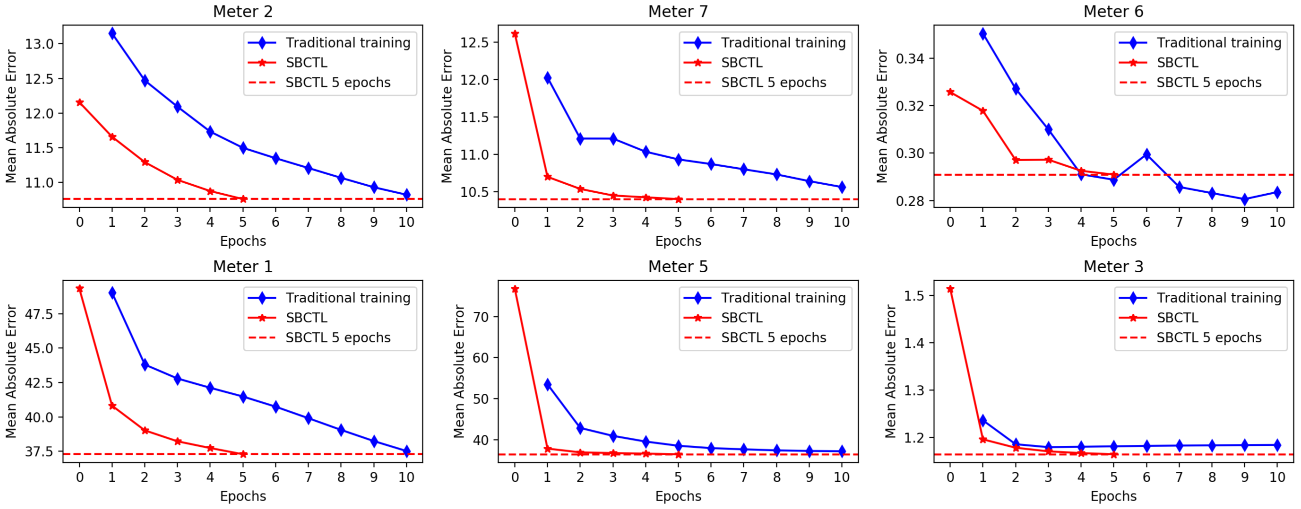

FIGURE 6: Experiment 1: Test set MAE for SBCTL and traditional ML.

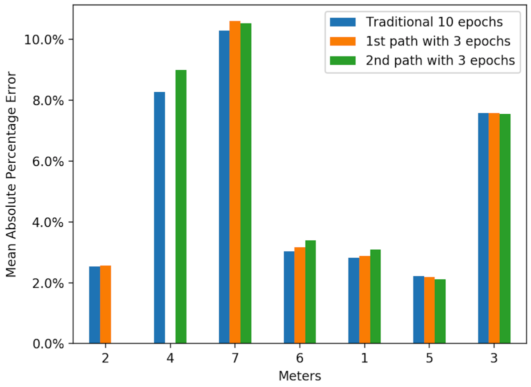

FIGURE 7: Experiment 1: Test set MAPE for the two SBCTL paths.

starting with meter 4 or with 2 as the initial meter. Irrelevant of the starting meter, the transfer path, Table 2, remained the same with the exception of the source and target reversal in the first row. Fig. 7 shows the comparison between the two SBCTL paths with 3 epochs and traditional ML: MAPE was used in contrast to MAE used in Fig. 6 to bring all errors to similar scales. Meters 2 and 4 are missing the bar for the path in which they were used as the initial meter and therefore trained in a traditional way. Both paths resulted in similar MAPE values; moreover, MAPE values were comparable to those achieved with traditional ML.

Overall, in experiment one, SBCTL achieved similar accuracy to traditional ML while taking only about a fraction of time.

C. EXPERIMENT TWO

This data set is larger; thus, the experiment was performed on a computer with 3.80 GHz Intel i7-9800X processor, 32 GB RAM, and NVIDIA GeForce RTX 2080 Ti graphics card. GPU acceleration was used for training ML models.

1) Data set

This experiment used an open source data set [34] containing readings from 20 meters recorded in the one-hour intervals. Readings from the same 487 consecutive days were taken for each meter: $24\times 487 = 11{,}688$ readings for each meter.

2) Experiment

The same process was used as in experiment one. Meter 7 had the same readings as meter 3 for all time steps; thus, meter 3 was removed from further evaluations. The chained transfer path for Euclidean distance is shown in Table 4.

3) Result

The starting meter for initialization *B* was the same as one of the meters in the initialization *A* starting pair. The mean MAPE and MAE across all meters for different distance metrics are compared in Fig. 8. Different similarity metrics resulted in different chained transfer paths with exception of Euclidean and Cosine distances which had the same path; thus, in Fig. 8 they share the same values. In all metrics, SBCTL out-performed the traditional machine learning with Euclidean/Cosine distance achieving the best accuracy.

SBCTL with initialization *B* and Euclidean distance is compared to traditional ML for each meter in Fig. 10; the

TABLE 4: Experiment Two: Chained Transfer Path

Step	Source	Target	Distance	Step	Source	Target	Distance
1	m_7	m_2	0.001	10	m_{19}	m_{17}	26.49
2	m_7	m_6	2.96	11	m_{19}	m_1	28.85
3	m_6	m_{20}	33.74	12	m_{20}	m_{13}	32.73
4	m_{20}	m_{18}	31.69	13	m_{16}	m_{12}	34.11
5	m_{18}	m_{19}	22.17	14	m_{12}	m_{11}	17.35
6	m_{18}	m_{16}	22.74	15	m_5	m_8	36.82
7	m_{18}	m_5	23.64	16	m_{13}	m_4	42.39
8	m_{19}	m_{15}	23.96	17	m_8	m_{10}	81.84
9	m_{19}	m_{14}	26.3	18	m_{10}	m_9	134.74

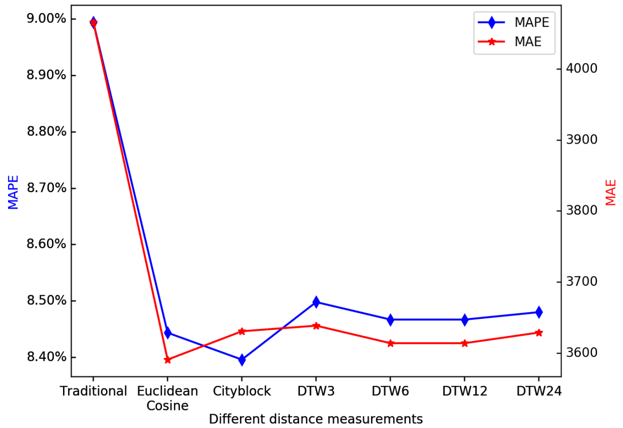

FIGURE 8: Experiment 2: Mean MAPE and MAE for different distance metrics.

order of meters in the figure follows the chained transfer path from Table 4.

Similar to graphs in experiment one, each graph shows the comparison for the specific meter not including the initial meter 7. In experiment two, MAPE is used in place of MAE, to use more similar scales in figures, nevertheless, MAE exhibited the same patterns. The horizontal line indicates SBCTL accuracy at 1 epoch as opposed to 3 epochs used in experiment one because most meters from this data set already achieve accuracy comparable to traditional ML in the first epoch. For all metes except meters 4 and 9, direct transfer, without any training with target data (epoch 0) already achieved comparable MAPE to traditional ML. After the first epoch, MAPE surpassed the traditional ML MAPE. For meter 9, SBCTL with 0 epoch exhibited high MAPE, but already after the first epoch, accuracy approached traditional ML values. For meter 4 traditional ML exhibited lower MAPE than SBCTL; however, it is important to note that for this meter MAPE is overall high, irrelevant of the approach used, what may be caused by high energy consumption variability.

Fig. 9 compares accuracy of traditional ML with SBCTL at the first and fifth epoch corresponding to the chained transfer path from Table 4. The first epoch was considered instead of the third epoch used for experiment one (Fig. 7), because most models achieved good accuracy already after the first epoch. It can be seen that SBCTL with one epoch achieved better accuracy than traditional ML with 10 epochs for all but two meters (4 and 9).

The average training time is shown in Table 5. Overall, in experiment two, SBCTL (initialization *B*, Euclidean distance) with one epoch achieved 0.55% reduction in MAPE and 474.88 in MAE compared to traditional ML while taking less then 1% of time.

D. EXPERIMENT THREE

This experiment was performed on a machine with Intel i7-9800X processor, 32 GB RAM, and four NVIDIA GeForce RTX 2080 Ti graphics cards. As in experiment two, GPU acceleration was used for training machine learning models.

TABLE 5: Experiment 2: Average Training Time

	Traditional			SBCTL	epoch		
	10	0	1	2	3	4	5
Time (s)	**94.53**	0	**0.88**	1.75	2.60	3.48	4.35
Std.Dev	0.19	0	0.01	0.02	0.02	0.03	0.04
Variance	0.04	0	0	0	0.001	0.001	0.001

1) Data set

An open source data set provided by the Building Data Genome project [35] was used in this experiment. This data set contains one year of hourly, whole building electrical meter data for 507 non-residential buildings. Meters with missing data and with less than one year of data were removed resulting in a set of 456 meters. For each meter there are 24(hours) * 365(days) = 8760 readings. Data were collected between 2010 and 2015 and, as data for each building spans only one year, the collection time periods vary among buildings. The meters are located in 9 different time zones and there are five primary use types: office, primary/secondary classroom, college laboratory, college classroom, and dormitory.

2) Experiment

The challenge with this data set is that it contains only one year of data and for SBCTL ideally, data set should have at least one year for training and additional data for testing. Nevertheless, the last 20% of data was used for testing and the first 80% for training prediction models and for calculating similarities. It is expected that this will not result in as high accuracy as if the hole year of data was used for training.

While in experiments one and two, accuracy could be visualized and observed for each meter separately (as in figures 6 and 10), this is more difficult for experiment three as it contains 456 meters. Thus, traditional machine learning

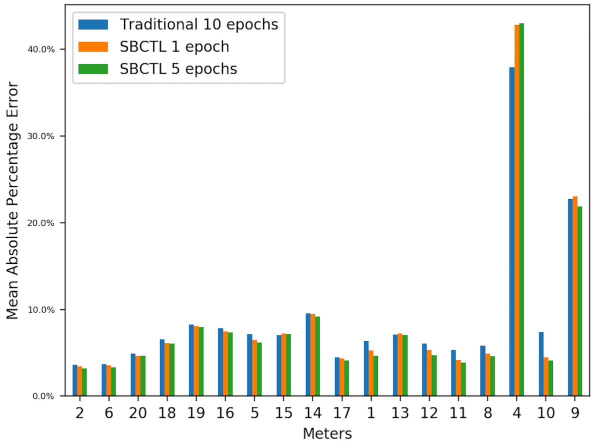

FIGURE 9: Experiment 2: Test set MAPE at first and fifth epoch.

This article has been accepted for publication in a future issue of this journal, but has not been fully edited. Content may change prior to final publication. Citation information: DOI 10.1109/ACCESS.2019.2943752, IEEE Access

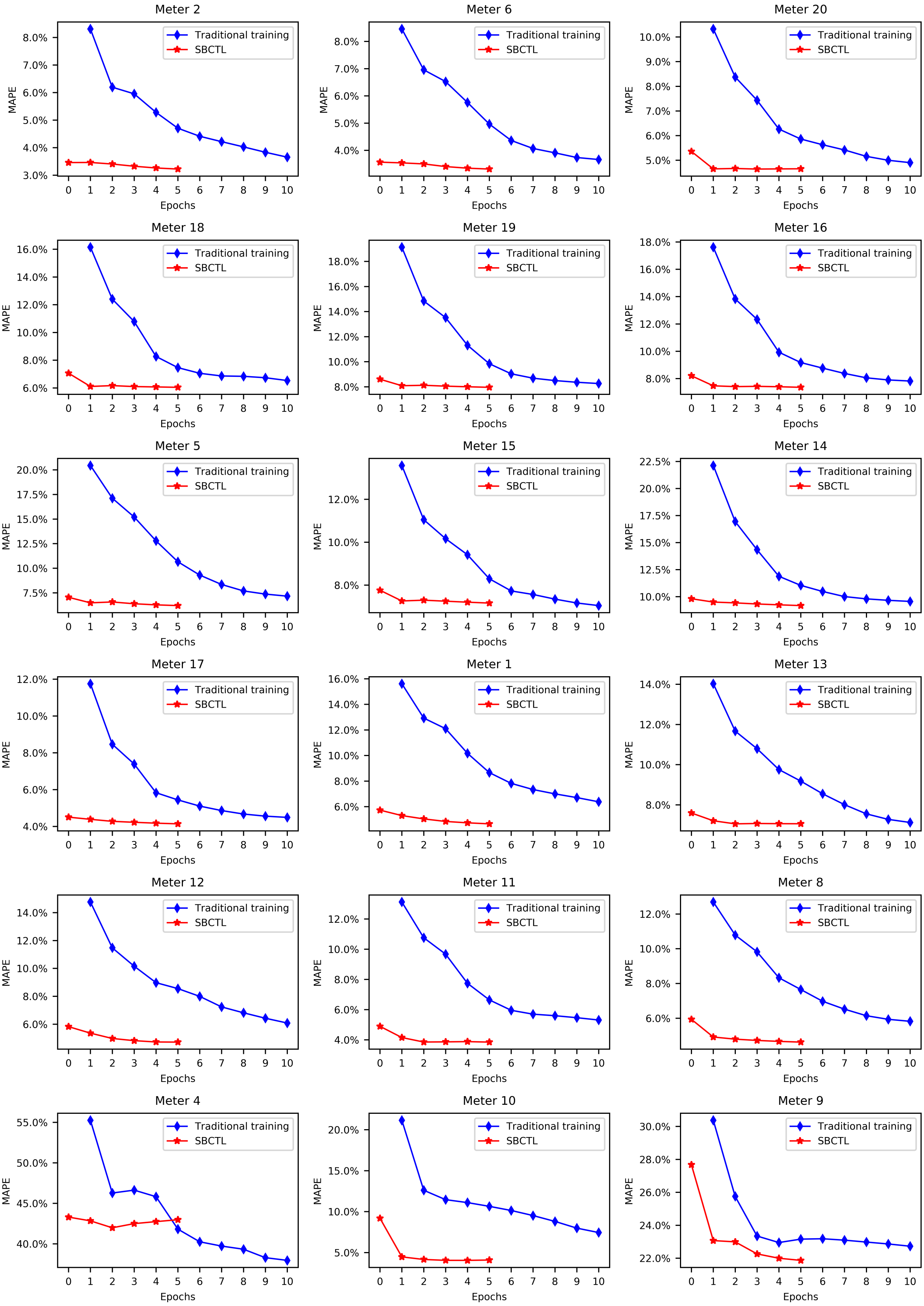

FIGURE 10: Experiment 2: Test set MAPE for SBCTL and traditional ML.

TABLE 6: Experiment 3: MAPE and MAE for initializations A and B, for each distance metrics

	Traditional	Euclidean	Cosine	Manhattan	DTW3	DTW 6	DTW12	DTW24
MAPE-A	30.1%	29.7%	30.6%	27.4%	33.0%	31.9%	36.5%	34.1%
MAPE-B	30.1%	25.1%	**22.8%**	25.2%	25.8%	27.4%	27.9%	25.9%
MAE-A	7.662	7.661	7.652	7.596	7.553	7.714	7.732	7.737
MAE-B	7.662	7.646	**7.500**	7.593	7.699	7.650	7.709	7.661

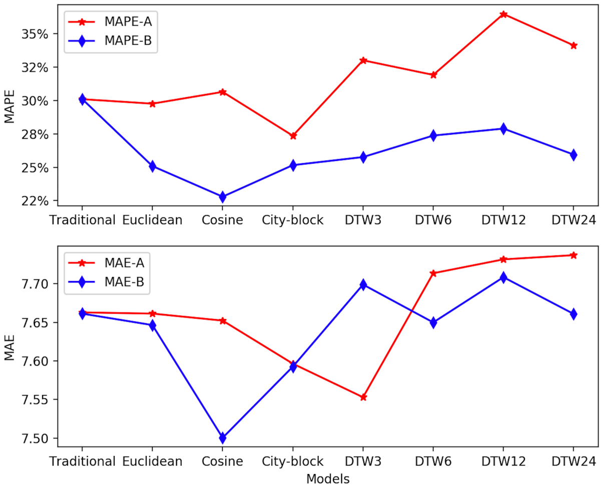

FIGURE 11: Experiment 3: MAPE and MAE for different initializations and distance metrics.

was performed with up to 30 epochs with early stopping when the loss function did not decrease in five consecutive epochs. This allows more epochs to achieve convergence, and, at the same time, helps remedy overfitting and avoids higher number of epochs if convergence is achieved earlier.

3) Result

In this experiment, transfer paths were different for the two initialization approaches *A* and *B*. Fig. 11 compares MAPE and MAE achieved with the two initializations for each of the distance metrics. The traditional approach does not have different initializations, thus accuracy for initializations *A* and *B* is the same. In terms of MAPE, initialization *B* outperformed initialization *A* for all distance metrics. This is slightly different for the MAE, where the initialization *A* achieved better accuracy for DTW with window of 3 time steps (DTW3). Nevertheless, irrelevant of the metrics used, the overall best model is with initialization *B* and Cosine distance.

Table 6 shows the data from Fig. 11 for further comparison. It can be observed that the best SBCTL model (initialization *B* with Cosine) achieved reduction of 7.3% in average MAPE and .163 in average MAE in comparison to traditional ML training.

The average elapsed time for all meters with the traditional ML and SBCTL are shown in Table 7. SBCTL used only about 2.6% of time needed to train the models in a traditional way.

TABLE 7: Experiment 3: Average Training Time

	Traditional			SBCTL	epoch		
	10	0	1	2	3	4	5
Time (s)	**30.33**	0	0.16	0.31	0.46	0.62	**0.77**
Std.Dev	10.24	0	0.01	0.03	0.04	0.05	0.06
Variance	104.78	0	0	0.001	0.002	0.003	0.004

E. DISCUSSION

In all three experiments, SBCTL achieved improved average accuracy in comparison to traditional ML. Overall, the best performing model was SBTCL with initialization *B* (from the center) and Euclidean distance. This can be observed from figures 8 and 11 for experiments one and two, whereas there was no difference among SBCTL approaches in the experiment one.

In experiments one and two, SBCTL models trained for 5 epoch achieved higher accuracy than traditional ML with 10 epoch. An exception was meter 4 in experiment two; nevertheless, that meter achieved low accuracy irrelevant of the approach, possibly because of high data variability. This demonstrated that transferring weights according to SBCTL approach is a promising direction for training a large number of energy forecasting models.

Note that in experiment two SBCTL needed only 1 epoch to achieve comparable results to traditional ML where it needed 3 epochs in experiment one. Moreover, in experiment two, even direct transfer without additional training (epoch 0) achieved good accuracy. The reason for this is a higher similarity between meters in experiment two. In experiment one, the lowest Euclidean distance was 135.2 (Table 2) and the mean was 182.65. Meanwhile, the lowest Euclidean distance in experiment two was 0.001 (Table 4) and mean was 34.58.

In all experiments, the time to train SBCTL models was only a fraction of time in comparison to traditional ML while they achieved comparable accuracy. Training time reduction depends on the number of epoch needed after the transfer what is impacted by the similarity between meters.

SBTCL requires all smart meter data sets to have the same sampling frequency or the data sets need to be preprocessed to convert them to the same frequency. If there are any missing data, they need to be imputed in the preparation step in order to enable the similarity calculations. As SBCTL transfers NN weights from one meter to another, and continues training from those weight, there is a possibility of the transferred model getting stuck in a local minimum. However, the presented experiments, even the third one with 456 meters, demonstrate high accuracy in spite of a possibility of a local minimum.

VI. CONCLUSION

Extensive smart meter deployments have created opportunities for energy forecasting on a large scale. Machine learning-based forecasting typically involves training the model with historical data from a single building and then using this model to infer consumption for the same building. As training is computationally intensive, it is not practical to train ML models individually for many meters.

This paper proposes Similarity-Based Chained Transfer Learning (SBCTL) to enable building neural network-based forecasting models for a large number of smart meters. The initial model is built in a traditional way whereas all other models use transfer learning in a chain-like manner. SBCTL is evaluated with three different data sets: in all experiments, SBCTL achieves similar accuracy to traditional ML training while taking only a fraction of time. The best results are achieved with Euclidean distance and starting from the meter closest to the center. As illustrated in experiments one and two, the SBCTL time depends on the number of epochs needed for convergence after the transfer. When meters are more similar in terms of their energy consumption profiles, SBCTL needs fewer epochs and thus, training time is shorter. The third experiment demonstrates that SBCTL maintains its high accuracy even with a data set of 456 meters.

Future work will further explore the impact of similarly on the number of epochs needed after the transfer. Moreover, possibility to transfer knowledge among data sets of different duration and with different reading intervals will also be explored.

REFERENCES

[1] Y. Wang, Q. Chen, T. Hong, and C. Kang, "Review of smart meter data analytics: Applications, methodologies, and challenges," IEEE Transactions on Smart Grid, 2018.

[2] X. Huang, S. H. Hong, and Y. Li, "Hour-ahead price based energy management scheme for industrial facilities," IEEE Transactions on Industrial Informatics, vol. 13, no. 6, pp. 2886–2898, 2017.

[3] D. Alahakoon and X. Yu, "Smart electricity meter data intelligence for future energy systems: A survey," IEEE Transactions on Industrial Informatics, vol. 12, no. 1, pp. 425–436, 2016.

[4] K. Amber, R. Ahmad, M. Aslam, A. Kousar, M. Usman, and M. Khan, "Intelligent techniques for forecasting electricity consumption of buildings," Energy, vol. 157, pp. 886–893, 2018.

[5] K. Hassanpouri Baesmat and A. Shiri, "A new combined method for future energy forecasting in electrical networks," International Transactions on Electrical Energy Systems, vol. 29, no. 3, p. e2749, 2019.

[6] K. Grolinger, M. A. Capretz, and L. Seewald, "Energy consumption prediction with big data: Balancing prediction accuracy and computational resources," in 2016 IEEE International Congress on Big Data, pp. 157–164, 2016.

[7] L. Sehovac, C. Nesen, and K. Grolinger, "Forecasting building energy consumption with deep learning: A sequence to sequence approach," in IEEE International Congress on Internet of Things, 2019.

[8] S. J. Pan and Q. Yang, "A survey on transfer learning," IEEE Transactions on knowledge and data engineering, vol. 22, no. 10, pp. 1345–1359, 2010.

[9] I. Goodfellow, Y. Bengio, and A. Courville, Deep Learning. MIT Press, 2016. http://www.deeplearningbook.org.

[10] S. Bouktif, A. Fiaz, A. Ouni, and M. Serhani, "Optimal deep learning LSTM model for electric load forecasting using feature selection and genetic algorithm: Comparison with machine learning approaches," Energies, vol. 11, no. 7, p. 1636, 2018.

[11] K. Cho, B. Van Merriënboer, C. Gulcehre, D. Bahdanau, F. Bougares, H. Schwenk, and Y. Bengio, "Learning phrase representations using RNN encoder-decoder for statistical machine translation," arXiv preprint arXiv:1406.1078, 2014.

[12] L. Tang, X. Wang, X. Wang, C. Shao, S. Liu, and S. Tian, "Long-term electricity consumption forecasting based on expert prediction and fuzzy bayesian theory," Energy, vol. 167, pp. 1144–1154, 2019.

[13] K. Grolinger, A. L'Heureux, M. A. Capretz, and L. Seewald, "Energy forecasting for event venues: Big data and prediction accuracy," Energy and Buildings, vol. 112, pp. 222–233, 2016.

[14] Y. Ma, P. Liu, Y. Cui, and S. Liu, "Proposed model employing ARIMA and RELM in urban energy consumption prediction," in 2018 International Symposium on Computer, Consumer and Control, pp. 465–468, 2018.

[15] K. Li, X. Xie, W. Xue, X. Dai, X. Chen, and X. Yang, "A hybrid teaching-learning artificial neural network for building electrical energy consumption prediction," Energy and Buildings, vol. 174, pp. 323–334, 2018.

[16] M. Khairalla, X. Ning, N. AL-Jallad, and M. El-Faroug, "Short-term forecasting for energy consumption through stacking heterogeneous ensemble learning model," Energies, vol. 11, no. 6, p. 1605, 2018.

[17] S. Han, Y.-h. Qiao, J. Yan, Y.-q. Liu, L. Li, and Z. Wang, "Mid-to-long term wind and photovoltaic power generation prediction based on copula function and long short term memory network," Applied Energy, vol. 239, pp. 181–191, 2019.

[18] R. Jiao, T. Zhang, Y. Jiang, and H. He, "Short-term non-residential load forecasting based on multiple sequences LSTM recurrent neural network," IEEE Access, vol. 6, pp. 59438–59448, 2018.

[19] D. L. Marino, K. Amarasinghe, and M. Manic, "Building energy load forecasting using deep neural networks," in 42nd Annual Conference of the IEEE Industrial Electronics Society, pp. 7046–7051, 2016.

[20] F. Zhu and L. Shao, "Weakly-supervised cross-domain dictionary learning for visual recognition," International Journal of Computer Vision, vol. 109, no. 1-2, pp. 42–59, 2014.

[21] W. Hu, Y. Qian, F. K. Soong, and Y. Wang, "Improved mispronunciation detection with deep neural network trained acoustic models and transfer learning based logistic regression classifiers," Speech Communication, vol. 67, pp. 154–166, 2015.

[22] Y. Ma, G. Luo, X. Zeng, and A. Chen, "Transfer learning for cross-company software defect prediction," Information and Software Technology, vol. 54, no. 3, pp. 248–256, 2012.

[23] J. Nam, S. J. Pan, and S. Kim, "Transfer defect learning," in 35th International Conference on Software Engineering, pp. 382–391, 2013.

[24] W. Li, L. Duan, D. Xu, and I. W. Tsang, "Learning with augmented features for supervised and semi-supervised heterogeneous domain adaptation," IEEE transactions on pattern analysis and machine intelligence, vol. 36, no. 6, pp. 1134–1148, 2014.

[25] A. S. Mozafari and M. Jamzad, "A SVM-based model-transferring method for heterogeneous domain adaptation," Pattern Recognition, vol. 56, pp. 142–158, 2016.

[26] A. Krizhevsky, I. Sutskever, and G. E. Hinton, "Imagenet classification with deep convolutional neural networks," in Advances in neural information processing systems, pp. 1097–1105, 2012.

[27] A. Menegola, M. Fornaciali, R. Pires, F. V. Bittencourt, S. Avila, and E. Valle, "Knowledge transfer for melanoma screening with deep learning," in IEEE 14th International Symposium on Biomedical Imaging, pp. 297–300, 2017.

[28] S. Lu, Z. Lu, and Y.-D. Zhang, "Pathological brain detection based on alexnet and transfer learning," Journal of computational science, vol. 30, pp. 41–47, 2019.

[29] E. Mocanu, P. H. Nguyen, W. L. Kling, and M. Gibescu, "Unsupervised energy prediction in a smart grid context using reinforcement cross-building transfer learning," Energy and Buildings, vol. 116, pp. 646–655, 2016.

[30] T. Grubinger, G. C. Chasparis, and T. Natschläger, "Generalized online transfer learning for climate control in residential buildings," Energy and Buildings, vol. 139, pp. 63–71, 2017.

[31] M. Ribeiro, K. Grolinger, H. F. ElYamany, W. A. Higashino, and M. A. Capretz, "Transfer learning with seasonal and trend adjustment for cross-building energy forecasting," Energy and Buildings, vol. 165, pp. 352–363, 2018.

[32] O. Abedinia, N. Amjady, and H. Zareipour, "A new feature selection technique for load and price forecast of electrical power systems," IEEE Transactions on Power Systems, vol. 32, no. 1, pp. 62–74, 2017.

[33] Z. Yu, Z. Niu, W. Tang, and Q. Wu, "Deep learning for daily peak load forecasting–a novel gated recurrent neural network combining dynamic time warping," IEEE Access, vol. 7, pp. 17184–17194, 2019.

[34] Kaggle, "Global Energy Forecasting Competition." https://www.kaggle.com/c/global-energy-forecasting-competition-2012-load-forecasting/data. Online: accessed May 2019.

[35] C. Miller and F. Meggers, "The building data genome project: An open, public data set from non-residential building electrical meters," Energy Procedia, vol. 122, pp. 439 – 444, 2017.